

Universal scaling properties of QCD close to the chiral limit*

OLAF KACZMAREK, FRITHJOF KARSCH,
ANIRBAN LAHIRI[†], CHRISTIAN SCHMIDT

Fakultät für Physik, Universität Bielefeld, D-33615 Bielefeld, Germany

We present a lattice QCD based determination of the chiral phase transition temperature in QCD with two massless (up and down) and one strange quark having its physical mass. We propose and calculate two novel estimators for the chiral transition temperature for several values of the light quark masses, corresponding to Goldstone pion masses in the range of $58 \text{ MeV} \lesssim m_\pi \lesssim 163 \text{ MeV}$. The chiral phase transition temperature is determined by extrapolating to vanishing pion mass using universal scaling relations. After thermodynamic, continuum and chiral extrapolations we find the chiral phase transition temperature $T_c^0 = 132_{-6}^{+3} \text{ MeV}$. We also show some preliminary calculations that use the conventional estimator for the pseudo-critical temperature and compare with the new estimators for T_c^0 . Furthermore, we show results for the ratio of the chiral order parameter and its susceptibility and argue that this ratio can be used to differentiate between $O(N)$ and Z_2 universality classes in a non-parametric manner.

PACS numbers: 11.10.Wx, 11.15.Ha, 12.38.Aw, 12.38.Gc, 12.38.Mh, 24.60.Ky, 25.75.Gz, 25.75.Nq

1. Introduction

By now it is well established that for physical values of light and strange quark masses QCD undergoes a smooth crossover from a low temperature hadronic phase to a high temperature partonic phase [1, 2]. The chiral crossover temperature has been determined in various numerical studies of lattice QCD [3, 4, 5, 6, 7]. On the other hand the order of the QCD transition in the chiral limit with two massless degenerate quarks has been a celebrated topic without any concrete conclusion, yet. It has been argued long back [8]

* Presented at workshop on Criticality in QCD and the Hadron Resonance Gas; 29-31 July 2020, Wrocław, Poland.

[†] Speaker

that “effective restoration” of $U(1)_A$, which is broken in vacuum, could play a very important role determining the order of the chiral phase transition for two massless flavors. When the $U(1)_A$ remains broken at the chiral transition temperature, the chiral transition is expected to belong to the $O(4)$ universality class [8] which is the most celebrated scenario till date. In case the $U(1)_A$ gets effectively restored at the chiral transition then the latter may become first order [8], although second order phase transition belonging to other 3-d universality classes could also become relevant [9, 10, 11, 12]. If the chiral transition is first order then there exists an endpoint, belonging to Z_2 universality class, at a non-zero value of light quark mass, $m_l^c > 0$ where the chiral susceptibility will diverge.

In this contribution we present the first lattice QCD based determination [15] of the chiral phase transition temperature. Since there is no direct evidence for a first order phase transition down to a quite small pion mass, we employ the $O(N)$ scaling to calculate the critical temperature for vanishing light quark masses. We introduce and present results for two novel estimators of T_c^0 which are reliable even for finite quark masses. We also present result for the ratio of the chiral order parameter and its susceptibility and argue that this ratio can be very effective in differentiating between $O(N)$ and Z_2 universality classes in a non-parametric manner.

2. Formalism

We start with the definition of the quark condensate,

$$\langle \bar{\psi}\psi \rangle_f = \frac{T}{V} \frac{\partial \ln Z(T, V, m_u, m_d, m_s)}{\partial m_f}. \quad (1)$$

In the chiral limit, the light quark chiral condensate $\langle \bar{\psi}\psi \rangle_l = (\langle \bar{\psi}\psi \rangle_u + \langle \bar{\psi}\psi \rangle_d)/2$, serves as an exact order parameter for the spontaneous breaking of chiral symmetry at low temperature. Additive and multiplicative renormalization have been taken care of by introducing [4] a combination of light and strange quark condensates,

$$M = 2 (m_s \langle \bar{\psi}\psi \rangle_l - m_l \langle \bar{\psi}\psi \rangle_s) / f_K^4, \quad (2)$$

where $f_K = 156.1(9)/\sqrt{2}$ MeV, is the kaon decay constant, used as a normalization constant. The chiral susceptibility is defined as,

$$\chi_M = m_s (\partial_{m_u} + \partial_{m_d}) M |_{m_u=m_d}. \quad (3)$$

Close to a 2^{nd} order phase transition, M and χ_M are expected to be described by universal finite-size scaling functions $f_G(z, z_L)$ and $f_\chi(z, z_L)$

[18],

$$\begin{aligned} M &= h^{1/\delta} f_G(z, z_L) + f_{sub}(T, H, L) , \\ \chi_M &= h_0^{-1} h^{1/\delta-1} f_\chi(z, z_L) + \tilde{f}_{sub}(T, H, L) , \end{aligned} \quad (4)$$

where the scaling variables in the arguments are defined as $z = t/h^{1/\beta\delta}$ and $z_L = l_0/(Lh^{\nu/\beta\delta})$, with $t = (T/T_c^0 - 1)/t_0$ denoting the reduced temperature; $h = H/h_0$ with $H = m_l/m_s$ being the symmetry breaking field, and L denoting the linear extent of the system, $L \equiv V^{1/3}$. The normalization constants t_0 , h_0 and l_0 appearing in definition of the scaling variables are non-universal parameters. $f_{sub}(T, H, L)$ and $\tilde{f}_{sub}(T, H, L)$ denote sub-leading contributions which arise due to contributions from corrections-to-scaling [13, 14] and regular terms, away from the critical point, for M and χ_M respectively.

For large enough system sizes, the peak in the scaling function $f_\chi(z, z_L)$ has been used as the usual estimator for the pseudo-critical temperature T_p , which scales as

$$T_p(H, L) = T_c^0 \left(1 + \frac{z_p(z_L)}{z_0} H^{1/\beta\delta} \right) + \text{sub-leading} , \quad (5)$$

with $z_0 = h_0^{1/\beta\delta}/t_0$. The universal quark mass dependence of T_p is described by the first term and ‘sub-leading’ represents contributions from corrections-to-scaling and regular terms. In principle, the situation is same for scaling of a temperature $T_X(H, L)$ defined at any fixed value z_X ($X = p$ in Eq. 5). Depending on the value of z_X/z_0 , $T_X(H, L)$ may change significantly within a given window of H , towards chiral limit [4]. This makes the chiral extrapolation complicated due to increasing importance of the contribution from the sub-leading terms. Here we consider two estimators [15, 16] for T_c^0 , defined close to or at $z = 0$, in the thermodynamic limit resulting in an order of magnitude smaller mass variation in Eq. 5. Pseudo-critical temperatures T_δ and T_{60} are defined through,

$$\frac{H\chi_M(T_\delta, H, L)}{M(T_\delta, H, L)} = \frac{1}{\delta} , \quad (6)$$

$$\chi_M(T_{60}, H) = 0.6\chi_M^{max} . \quad (7)$$

Since $z_\delta \equiv z_\delta(0) = 0$ and $z_{60} \equiv z_{60}(0) \simeq 0$, These pseudo-critical temperatures, T_δ and T_{60} , give already a reasonable estimate of T_c^0 for non-zero H and L^{-1} . Forms of universal functions $z_X(z_L)$ along with the optimal parameterized form can be found in Ref.[19], for the 3-d, $O(4)$ universality class. Here we present the calculation of T_c^0 through T_δ and T_{60} . Details of

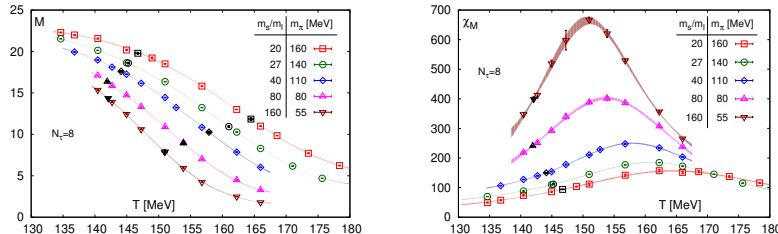


Fig. 1. Right: Quark mass dependence of chiral condensate (left) and the chiral susceptibility (right) on lattices with temporal extent $N_\tau = 8$ for several values of the light quark masses. The spatial lattices extent N_σ is increased as the light quark mass decreases: $N_\sigma = 32$ ($H^{-1} = 20, 27$), 40 ($H^{-1} = 40$), 56 ($H^{-1} = 80, 160$). Black symbols in the susceptibility plot mark the points corresponding to 60% of the peak height and the corresponding values of condensate has also been marked with black symbols for low temperatures and the condensates at the peak position of the susceptibility have also been depicted by bunch of black points at higher temperatures. Right panel plot is taken from [15].

the calculational set-up can be found in Ref.[15]. Ignoring corrections-to-scaling and keeping in f_{sub} only the leading T -independent, infinite volume regular contribution proportional to H , we then find for the pseudo-critical temperatures [15],

$$T_X(H, L) = T_c^0 \left(1 + \left(\frac{z_X(z_L)}{z_0} \right) H^{1/\beta\delta} \right) + c_X H^{1-1/\delta+1/\beta\delta}, \quad X = \delta, 60. \quad (8)$$

Here we also present the results for the ratio of M and χ_M and we argue that this ratio can be used to study the difference between the $O(N)$ and Z_2 universality classes, through a non-parametric comparison. In the infinite volume limit, following Eq. 4 one can write:

$$\frac{M}{\chi_M} \Big|_{T_X, H} = \frac{f_G}{f_\chi} \Big|_{z_X} H + c_r h_0^{1/\delta} H^{2-1/\delta} \left[\frac{f_G}{f_\chi} \left(\frac{1}{f_G} - \frac{1}{f_\chi} \right) \right] \Big|_{z_X} \quad (9)$$

where the first term is the universal part and the second term is a regular contribution which has been calculated by taking $f_{sub} = c_r H$ in Eq. 4. We will calculate the ratio in the LHS of Eq. 9 in the thermodynamic limit at different temperatures like T_p and T_{60} and compare with that from scaling expectation of RHS, where $f_G(z)$ and $f_\chi(z)$ will be numbers fixed by the universality class. As can be seen from Eq. 9 a comparison without the regular term is parameter free. If a second order Z_2 endpoint exists at some finite quark mass, H_c , then we have to replace H by $H - H_c$ in the RHS of Eq. 9.

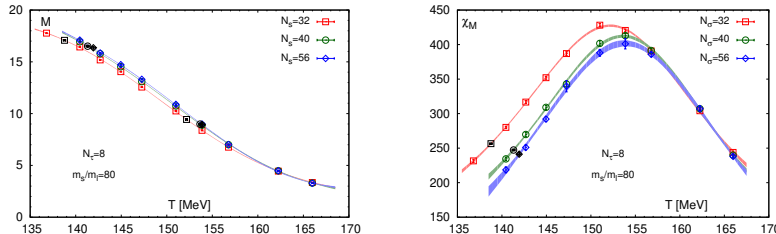


Fig. 2. Left: Volume dependence of the chiral condensate on lattices with temporal extent $N_\tau = 8$ for three different spatial lattice sizes at $H = 1/80$. Bunch of three black symbols at higher and lower temperatures denote M at T_p and for T_{60} , respectively. Right: Volume dependence of the chiral susceptibility on lattices with temporal extent $N_\tau = 8$ for three different spatial lattice sizes at $H = 1/80$. Black symbols mark the points corresponding to 60% of the peak height. Right panel plot is taken from [15].

3. Results

We start with the results for M for different values of H which is shown in Fig. 1 (left) for lattices of size $N_\sigma^3 \times N_\tau$ with $N_\tau = 8$. One can see clearly that M decreases with decreasing H and the crossover becomes sharper towards smaller H . In Fig. 1 (right) we show the chiral susceptibility for lattices as for Fig. 1 (left). The apparent increase of peak height is visible with decreasing H and this is consistent with the expected behavior, $\chi_M^{max} \sim H^{1/\delta-1} + \text{const.}$, with $\delta \simeq 4.8$, although within rather large uncertainty which restricts a precise determination of δ .

In Fig. 2 (left) we show the volume dependence of the order parameter for $H = 1/80$ on lattices with $N_\tau = 8$ and for different aspect ratios, $N_\sigma/N_\tau = 4, 5$ and 7 . One can see that M increases and saturates when approaching the thermodynamic limit. This is found as a basic feature in $O(4)$ finite size scaling studies [18] when there is a second order phase transition for vanishing external field. In Fig. 2 (right) we show the volume dependence for the same lattices as for Fig. 2 (left). Similar results have also been obtained for $N_\tau = 6$ and 12 . It is important to note that χ_M^{max} decreases slightly with increasing volume, contrary to what one would expect to find at or close to a 1st order phase transition. In fact this trend also seems to be consistent with the behavior seen for $O(4)$ universality class finite-size scaling functions [18]. Our current results, thus, suggest a continuous phase transition at $H_c = 0$.

Using the results of M and χ_M we have constructed the ratio $H\chi_M/M$ for lattices with different spatial extents and several values of the light quark masses. In Fig. 3 (left) this ratio has been shown for the $N_\tau = 12$ lattices

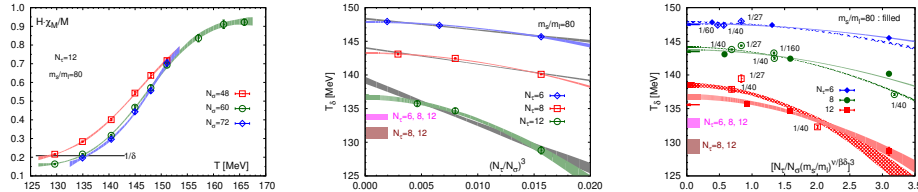


Fig. 3. Left: The ratio $H\chi_M/M$ versus temperature for $N_\tau = 12$, $m_l/m_s = 1/80$ and different spatial volumes. Middle: Infinite volume extrapolations based on an $O(4)$ finite-size scaling function (colored bands) and fits linear in $1/V$ (grey bands). Horizontal bars show the continuum extrapolated results for $H = 1/80$. Right: Finite size scaling fits for T_δ based on all data for $H \leq 1/27$ and all available volumes. Arrows show chiral limit results at fixed N_τ and horizontal bars show the continuum extrapolated results for $H = 0$. Figures are taken from [15].

with $H = 1/80$, as a typical example. Colored bands are interpolations to the data and the crossings with the horizontal line at $1/\delta$ define $T_\delta(H, L)$. We extrapolate $T_\delta(H, L)$ for a fixed H by two methods: (1) using the $O(4)$ scaling function following Eq. 8 where the volume correction is roughly $1/V^2$ [19] and (2) assuming $1/V$ correction which is the case if the volume correction is of regular origin. The resulting volume extrapolations are shown in Fig. 3 (middle) where it can be seen that the data seems to reach the thermodynamic limit faster than $1/V$. The difference between these two extrapolations to the thermodynamic limit serves as one component of the systematic uncertainty. The same procedure has been followed for all three different N_τ values and then the continuum extrapolation of these infinite volume results is performed with and without $N_\tau = 6$ which gives a second source to the systematic uncertainty. These continuum extrapolated results are shown in Fig. 3 (middle) by horizontal bands with different colors. The same set of analyses have also been performed for $H = 1/40$. Finally, we extrapolate the $T_\delta(H, \infty)$ for $H = 1/40$ and $1/80$ to the chiral limit using Eq. 8, putting $z_\delta(0) = 0$. Results obtained from these extrapolation chains, with the thermodynamic limit results obtained either through $O(4)$ or $1/V$ ansatz, and continuum limit extrapolations with and without $N_\tau = 6$, lead to chiral phase transition temperatures T_c^0 in the range (128-135) MeV.

Since from Fig. 3 (middle) we can see that the $O(4)$ scaling ansatz is already working quite well for finite lattice spacing, we attempt a joint extrapolation to the chiral and thermodynamic limit using results for all masses and on all available volumes, through $O(4)$ finite-size scaling function. The resulting extrapolations for three different N_τ are shown in Fig. 3 (right) where we show the extrapolation only for $H = 1/40$ and $H = 1/80$ for better readability of the plot. Noticeably for $H = 1/80$, these bands

compare well with the fits shown in Fig. 3 (middle). Colored arrows show the chiral limit results for each N_τ , in the thermodynamic limit. As a final step, the continuum extrapolation has been performed again with and without the $N_\tau = 6$ result. The results are shown by the horizontal bars in different colors in Fig. 3 (right). Results for T_c^0 , obtained by this method, are also shown in Fig. 4 and they are found to be in complete agreement with the corresponding numbers when the continuum limit has been taken before the chiral limit.

For T_{60} same set of analyses has been done as for T_δ and, as can be seen from Fig. 4, the resulting T_c^0 numbers from analyses of T_{60} agree within 1% with the same obtained from T_δ analyses. Leaving out $N_\tau = 6$ numbers systematically gives a 2-3 MeV decrease of T_c^0 , reflected in the displacement of the two colored bands in Fig. 4. Out of all the above-mentioned analyses we finally quote the chiral phase transition temperature,

$$T_c^0 = 132^{+3}_{-6} \text{ MeV} . \quad (10)$$

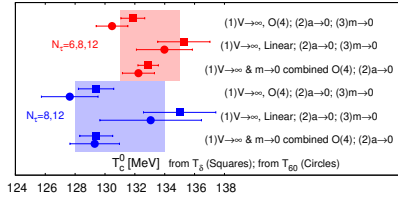


Fig. 4. Summary of fit results. The order of different limits taken, described in the main text, is written beside each pair of closest points. Figure is taken from [15].

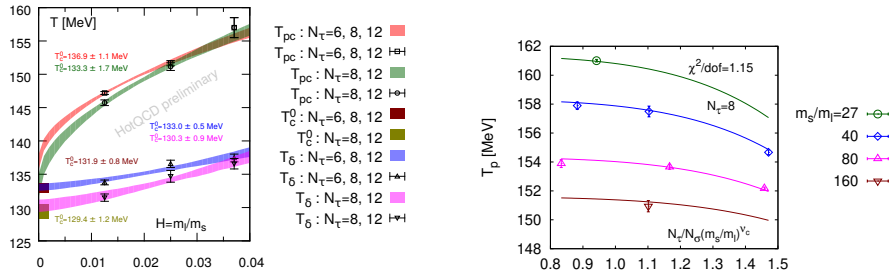


Fig. 5. Left: Comparison of chiral extrapolation of T_δ and T_p . Results for $H = 1/27$ is from lattices with aspect ratio 4 only. Horizontal bands represent the T_c^0 obtained from the T_δ analyses [15] without including $H = 1/27$. Right: Joint chiral and infinite volume extrapolation of T_p which gives $T_c^0 = 145.6(3)$ MeV for $N_\tau = 8$.

For completeness we also carried out the analyses for the peak position of the chiral susceptibility, *i.e.* T_p . Here also we first take the thermodynamic limit and then the continuum limit. Results for continuum extrapolated $T_p(H, \infty)$ are shown in Fig. 5 (left). For the extrapolation of T_p we could not include the sub-leading contributions, which is of course, important.

Including such a term with the three H values at our disposal, makes the chiral extrapolation way less controlled. Apparently the T_c^0 obtained from the extrapolations of T_p , even without a regular contribution, are in agreement with the same from T_δ within 95% confidence. The inclusion of a regular term will presumably make the agreement even better. Inclusion of $N_\tau = 6$ results, as usual gives systematically higher T_p , similar to the case of T_δ , as mentioned earlier. The numbers in Fig. 5 (left) are preliminary. Here we also show the T_p and T_δ for $H = 1/27$, for lattices with aspect ratio 4 only, for which finite volume effects have been estimated to be similar to the magnitude of the present uncertainty. This can be seen from Fig. 5 (right) where we have shown the joint chiral and thermodynamic limit extrapolation for $N_\tau = 8$ using the $O(4)$ finite size scaling functions. A similar analysis has also been carried out for $N_\tau = 6$ and 12. A continuum extrapolation then gives T_c^0 consistent with Fig. 5 (left) and other estimates within 95% confidence.

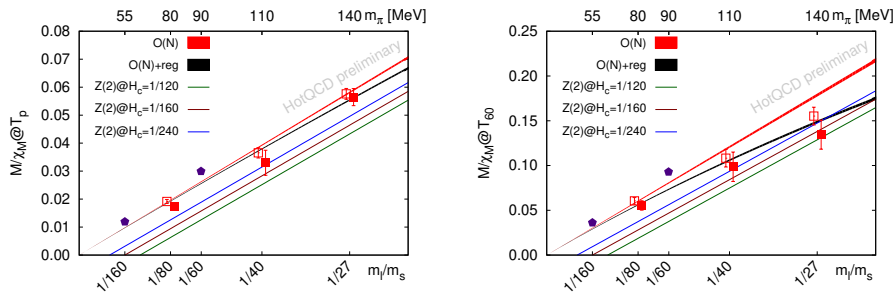


Fig. 6. Mass scaling of the ratio of M and χ_M at the peak (left) and at the 60% of the peak (right). The bands (hardly distinguishable from thick lines) are not fits and the width of the bands are due to the difference between $O(4)$ and $O(2)$ and for that reason the band collectively represented as $O(N)$. The squares represent the continuum extrapolated (open: with $N_\tau = 6$ and filled: without $N_\tau = 6$) results and the pentagons represent results for $N_\tau = 6$ and 8 with $H = 1/60$ and $1/160$, respectively.

Next we show in Fig. 6 left and right results for the ratio of M and χ_M evaluated at different temperatures, *i.e.* T_p and T_{60} , respectively. As discussed earlier this ratio gives a handle to compare the QCD results with results for different universality classes in a non-parametric way. We first calculate the ratio M/χ_M at the specified temperatures on different volumes for a fixed mass and fixed N_τ . We have already seen in Fig. 2 (left) and Fig. 2 (right) that the volume dependences of M and χ_M are very small both at T_p and T_{60} . As a result the volume dependence of the ratio M/χ_M is also found to be small and in most of the cases a linear volume extrapolation

gives the thermodynamic limit result which is in good agreement with that from the largest volume available. As usual for $H = 1/27$ we show the result for aspect ratio 4 and for this ratio we did not apply estimated correction because of the above-mentioned reason. Next we continuum extrapolate the ratio for a fixed H and these continuum extrapolated results are depicted in Fig. 6. For $H = 1/60$ and $1/160$ we have results only for $N_\tau = 6$ and 8, respectively. Like in other cases we checked the systematic uncertainty in the continuum extrapolation by including and excluding $N_\tau = 6$ results. In Fig. 6 we show the scaling expectations for $O(4)$ (relevant for continuum extrapolated cases) and $O(2)$ (relevant for results obtained with a finite lattice spacing) universality classes following Eq. 9. Expectations based on both universality classes differ little and are plotted together as a band denoted as $O(N)$. For the regular part of Eq. 9 we did not fit the coefficient c_r from the M/χ_M ratio. For our preliminary comparison we rather took the values of c_r and h_0 from the fit of M and χ_M . This seems to describe the data quite satisfactorily up to physical masses. In Fig. 6 one can see that the effect of a regular term is more important at T_{60} compared to T_p which seems to be counter-intuitive. Since the contribution of a (T -independent) regular term compared to the singular contribution rises for M and decreases for χ_M when one goes from T_{60} to T_p , a depreciation of the regular contribution of the ratio M/χ_M happens, which can be realized by looking at Eq. 9. We also show the scaling expectations for Z_2 universality class for different values of H_c . Of course, when there is a Z_2 endpoint at some non-vanishing H_c , then M , defined in Eq. 1 is not an exact order parameter anymore [20, 21]. Although one has to keep in mind that the mixing between magnetization like and energy like operators becomes smaller when H_c decreases. Fig. 6 apparently shows that with the current calculations, the existence of a Z_2 endpoint is unlikely down to $H_c = 1/240$ corresponding to $m_\pi \sim 45$ MeV.

4. Conclusions

Based on two novel estimators, we have calculated the chiral phase transition temperature in QCD with two massless light quarks and a physical strange quark. Eq. 10 lists our thermodynamic-, continuum- and chiral-extrapolated result for the chiral phase transition temperature, which is about 25 MeV smaller than the pseudo-critical (crossover) temperature, T_{pc} for physical values of the light and strange quark masses. Preliminary calculation of T_c^0 from the peak positions gives results which are in agreement within 95% confidence with the results from new estimators. We also showed the results for the ratio of the chiral condensate and chiral susceptibility which we used to differentiate between $O(N)$ and Z_2 universality classes in a non-parametric manner and we found that the existence of sec-

ond order endpoint belonging to Z_2 universality class seems to be unlikely down to $m_\pi \sim 45$ MeV.

5. Acknowledgement

This work was supported by the Deutsche Forschungsgemeinschaft (DFG) through Grant No. 315477589-TRR 211 and by Grant No. 05P18PBCA1 of the German Bundesministerium für Bildung und Forschung.

REFERENCES

- [1] Y. Aoki, G. Endrodi, Z. Fodor, S. D. Katz and K. K. Szabo, *Nature* **443**, 675-678 (2006).
- [2] for a recent review see: H. T. Ding, F. Karsch and S. Mukherjee, *Int. J. Mod. Phys. E* **24**, no. 10, 1530007 (2015).
- [3] Y. Aoki, S. Borsanyi, S. Durr, Z. Fodor, S. D. Katz, S. Krieg and K. K. Szabo, *JHEP* **0906**, 088 (2009).
- [4] A. Bazavov *et al.*, *Phys. Rev. D* **85**, 054503 (2012).
- [5] C. Bonati, M. D’Elia, M. Mariti, M. Mesiti, F. Negro and F. Sanfilippo, *Phys. Rev. D* **92**, 054503 (2015).
- [6] A. Bazavov *et al.* [HotQCD Collaboration], *Phys. Lett. B* **795** 15 (2019).
- [7] S. Borsanyi, Z. Fodor, J. N. Guenther, R. Kara, S. D. Katz, P. Parotto, A. Pasztor, C. Ratti and K. K. Szabo, *Phys. Rev. Lett.* **125**, 052001 (2020).
- [8] R. D. Pisarski and F. Wilczek, *Phys. Rev. D* **29**, 338 (1984).
- [9] A. Butti, A. Pelissetto and E. Vicari, *JHEP* **08**, 029 (2003).
- [10] M. Grahl and D. H. Rischke, *Phys. Rev. D* **88**, 056014 (2013).
- [11] A. Pelissetto and E. Vicari, *Phys. Rev. D* **88**, 105018 (2013).
- [12] T. Sato and N. Yamada, *Phys. Rev. D* **91**, 034025 (2015).
- [13] M. Hasenbusch, *J. Phys. A* **34**, 8221 (2001).
- [14] J. Engels, S. Holtmann, T. Mendes and T. Schulze, *Phys. Lett. B* **492**, 219 (2000).
- [15] H. T. Ding *et al.* [HotQCD Collaboration], *Phys. Rev. Lett.* **123**, 062002 (2019).
- [16] H.-T. Ding, P. Hegde, F. Karsch, A. Lahiri, S.-T. Li, S. Mukherjee and P. Petreczky, *Nucl. Phys. A* **982**, 211 (2019).
- [17] F. Karsch and E. Laermann, *Phys. Rev. D* **50**, 6954 (1994).
- [18] J. Engels and F. Karsch, *Phys. Rev. D* **90**, 014501 (2014).
- [19] O. Kaczmarek, F. Karsch, A. Lahiri, L. Mazur and C. Schmidt, [arXiv:2003.07920 [hep-lat]].
- [20] F. Karsch and S. Stickan, *Phys. Lett. B* **488**, 319-325 (2000).
- [21] F. Karsch, E. Laermann and C. Schmidt, *Phys. Lett. B* **520**, 41-49 (2001).